In-motion Inspection of Obstacles around Railways
by a Highly Accurate Laser-sectioning Method

Y. Jin*, Y. Goto*, H. Naito*, Y. Aono* and A. Iwake**

* Kobe Steel. Ltd. ; 1-5-5, Takatsukadai, Nishi-ku, Kobe, 651-22 Japan
** Cenyral Japan Railway Co. ; 1-6-5, Marunouti, Chiyoda-ku, Tokyou, 100 Japan

ABSTRACT

Nowadays, the automatization of railway maintenance work is a firm requirement. In order to respond in part to this requirement, a practical obstacle detecting system based on an original laser-sectioning method has been developed.

It was confirmed that the calibration for the obstacle detection was performed to an accuracy of more than 5 mm. Moreover, a theoretical estimation predicted that dynamic errors should be rejected to less than 5 mm by detection of rails.

A field test confirmed a sufficiently high sensibility of actual facilities detection at a running speed of 4 0km/h.

It is considered that the most advanced obstacle-detecting system for railways has been provided by this development.

INTRODUCTION

In railway maintenance works, observations for safety and facility inspections are still completely reliant upon human labour and modernization is highly desirable[1].

In recent years, laser-sectioning methods have been succesfully applied in various industrial fields[2]~[4]. Many attempts have been made to automatize railway inspection. The electrical inspecting vehicles[5], a computer system managing tunnel profile data[6] and Vehicle riding systems practical for large track areas[7],[8]. However, an in-motion inspection system for a wide area such as all around the railway has not been achieved till now.

The authors have developed an advanced light-sectioning method[9]. In this paper, we chiefly describe the error estimations of the system developed for practical use[10].

DESIGN OVERVIEW

One of the objectives of the system is in-motion inspection of facilities such as tunnels and platforms. This means real-time measurements of the locations and profiles, and judgements as to whether the construction gauge has been invaded or not. The construction gauge, prescribed by statute, is the boundary inside which no objects must be located.

In-motion inspection of railways requires a system with the characteristics of ① high accuracy, 10~20mm consistent with a wide view of total width 10m, ② real-time response, ③ freedom from fluctuations in running up to 4 0km/h, ④ missless for obstacles and ⑤ freedom from interference from the fluorescent lamps which railway facilities are equipped with. The system was designed around the above guidelines.

PRINCIPLE

Measurement Technique : The measurement is based on the advanced laser-sectioning method using originally developed H. V. D. (Horizontally-Vertically Different powered) imaging optics as shown in Fig.1. A laser sheet forms a light stripe on the object face corresponding to a sectional profile of the object. A high resolution cannot be achieved using a wide angle lens and a sufficiently wide view cannot be obtained with a telephoto lens. A H. V. D. imaging optics fulfills both characteristics of a wide view and a high resolution. As a result, a three-fold improvement range accuracy was achieved.
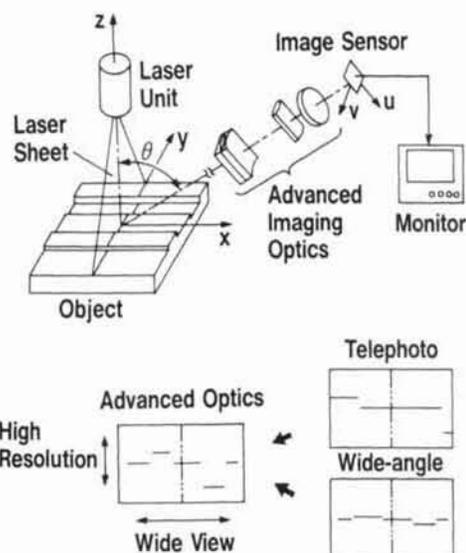

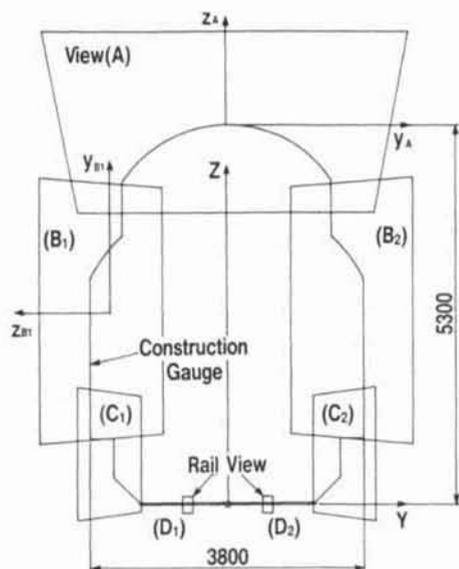Fig.1 Advanced Laser-Sectioning Method
with High Resolution and Wide View

Fig.2 Inspection View Fields and
the Construction Gauge

Fig.3 Calibration Target
for Views around the
Construction Gauge

Fig.4
Calibration
Target for
Rail Views

A laser-sectioning profile(y, z) can be obtained
from an image profile (u, v) on the image plane of
the sensor using the following formula.

$$y = \frac{(m_u+1)\cdot f_u}{m_u\cdot(m_u+1)\cdot f_u\cdot\sin\theta + m_u\cdot u\cdot\cos\theta}\cdot u \quad (1)$$

$$z = \frac{(m_v+1)\cdot f_v - m_v\cdot y\cdot\cos\theta}{m_v\cdot(m_v+1)\cdot f_v}\cdot v \quad (2)$$

Where, m_u and m_v are imaging magnifications($\ll 1$),
f_u and f_v are focal lengths of the H.V.D optics
and θ is the angle between light-sheet and optical
axis of camera. In the case of our system, resolu-
tions of the image sensor are $\varepsilon_u=16\,\mu m$, $\varepsilon_v=26\,\mu m$
(field mode) and focal lengths of H.V.D. optics are
$f_u=25mm$, $f_v=8.3mm$, although $f_u=f_v$ in an ordi-
nal case. The imaging resolution of the optics was
optimized to within $10\,\mu m$ on the image plane.

The view fields of the inspection are shown in
Fig.2 with the construction gauge. The five origi-
nal laser-sectioning systems cover the hole inspec-
tion area and two ordinary systems cover the rails.
As to a typical view field (B), $m_u=0.0057$, $m_v=
0.0017$ and $\theta=65°$. The size of the view along the
boundary is 3.9m and the resolution of range mea-
surement is estimated as 2.9mm from the formula (2).

Calibration : Two kinds of systematic error, which
occupy significant parts of static errors, must be
calibrated. The first kind of error is caused by
parameters m_u, m_v, f_u, f_v and θ. The other kind
of error is caused by a slight imaging distortion
formed by optical aberrations of H.V.D. optics, al-
though the imaging resolution is sufficiently high.

All static errors were calibrated inclusively
using calibration targets. Fig.3 shows a test tar-
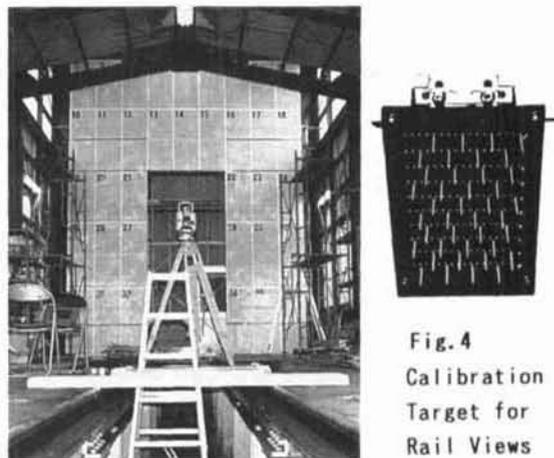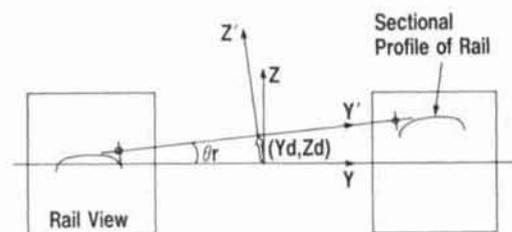get for the view all around the construction gauge.

Fig.5 Detection of the System Fluctuation
by Rail Position Measurement

The target is furnished with about fifty pins of di-
ameter 4 mm every view field. Fig.4 shows 1.5 mm
diameter one for the rail views. The target boards
stand parallel to the laser-sheet and all pins gen-
erate test points by a laser-sheet irradiation. The
locations of all pins (y_{ri}, z_{ri}) were previously
measured with accuracies better than 3 mm using a
high resolution theodolite(WILD TC-1600: 3 arcsec.)
and converted into the data (u_{ri}, v_{ri}) using the
formulae (1) and (2) reversely.

Raw image data (u_m, v_m), measured by the laser-
sectioning method and accompanied by systematic
error, should be calibrated into data (u_c, v_c) by
adequate calibration functions ($f(u,v)$ and $g(u,v)$)
and further converted into location data (y_c, z_c)
by the formulae (1)and(2). The functions of $f(u,v)$
and $g(u,v)$ were expressed intentionally with four-
th order polynominals as shown in formulae (3)and(4),
because the above-mentioned systematic errors were
estimated to be sufficiently corrected.

$$u = f(u,v)$$
$$= a_0+(a_1\cdot u+a_2\cdot v)+(a_3\cdot u^2+a_4\cdot u\cdot v+a_5\cdot v^2)$$
$$+(a_6\cdot u^3+\cdots\cdots+a_{15}\cdot v^4) \quad (3)$$

$$v = g(u,v)$$
$$= b_0+(b_1\cdot u+b_2\cdot v)+(b_3\cdot u^2+b_4\cdot u\cdot v+b_5\cdot v^2)$$
$$+(b_6\cdot u^3+\cdots\cdots+b_{15}\cdot v^4) \quad (4)$$
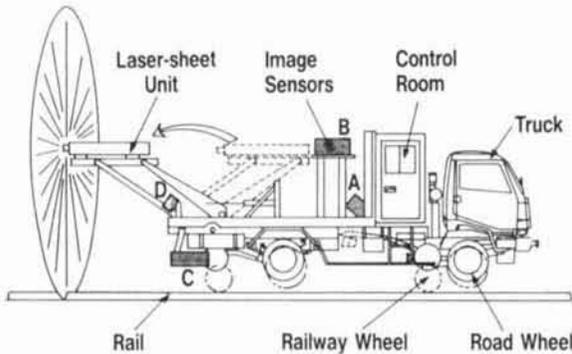
Fig.6 Outlook of the Inspection System

Fig.7 Configuration of the Inspection System

Image Processor

Fig.8 Block Diagram of the Image Processor

Table.1 $3-\sigma$ Deviations of the Calibrated Data from Real Values in four types of views

Target	Quantity	A	B	C	D
Test	$u_c - u_r$ (μm)	15	19	25	21
Pins	$y_c - y_r$ (mm)	3.9	3.8	2.5	0.52
Linear	$y_c - y_r$ (mm)	5.1	4.8	3.6	—

Thus, the number of test points 50 every view field was estimated to be sufficient. The coefficients a_i and b_i were determined using the least squares method.

Dynamic Error Correction : The final purpose of the system is in-motion obstacle detection and so the range values from vehicles are significant. The dynamic range errors are mostly caused by displacements $Y_d(t)$, $Z_d(t)$ and a rolling $\theta_r(t)$ of the sensing system[10]. The $Y_d(t)$, $Z_d(t)$ and $\theta_r(t)$ are detected from the sectional profiles of rails in the view fields (D_1) and (D_2), as shown in Fig.5. Thus the measurement becomes free from the fluctuations of the sensing system.

SYSTEM DESCRIPTION

The hole system, shown in Fig.6, comprises a sensing system, a data processing system and a truck. As known from the system configuration indicated in Fig.7, the sensing system comprises a laser-sheet unit and seven image sensor units, corresponding to the five inspection views and two rail views in Fig.2 respectively.

The laser-sheet unit is equipped with a continuous high-power laser diode(Spectra Diode Labs; 3 W, 8 00nm), collimating optics and a cone mirror held with a cylindrical window. A 360° spread laser-sheet, sent out from the unit, continuously irradiates the seven view fields shown in Fig.2.
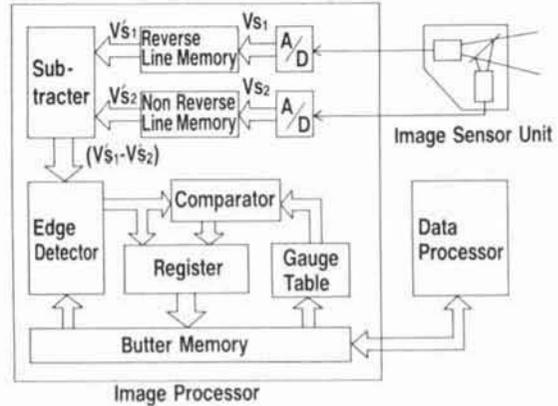
Each image sensor unit, for the five inspection

views, contains two CCD image sensors with H.V.D optics, in order to reject the fluorescent lamp images. One of them detects the laser-sectioning images, together with unwanted fluorescent lamp images. The other detects only the fluorescent lamp images.

The image processing system is set up in a control room and composed of seven image processors and a data processor. As can be seen from the sensing and processing block diagram shown in Fig.8, the image subtractors reject the fluorecent lamp images and the edge detectors detect the laser-sectional profiles in a speed of 16.7msec a video field. The correction of dynamic errors are performed by the data processor.

A 4 ton capacity truck carries the system described above and runs on both railways and conventional roads.

ERROR ESTIMATION

Static Errors: A static error is chiefly caused by ① a image sensor resolution, ② calibration errors of test pins, ③ image distortion of H.V.D. optics and ④ errors of (f, m, θ) used in formulae (1)and(2). The calibration mentioned above corrects the systematic errors of ③and④, but cannot reject the random errors of ①and②.

The above random errors cause statistical dispersions of the differences of calibrated data(u_c, v_c) from the real values (u_r, v_r). The $3-\sigma$ statistical deviations of$(u_c - u_r)$, obtained for about fifty test pins each view, are listed in Table.1 with them of $(y_c - y_r)$. The values are reasonably close to a
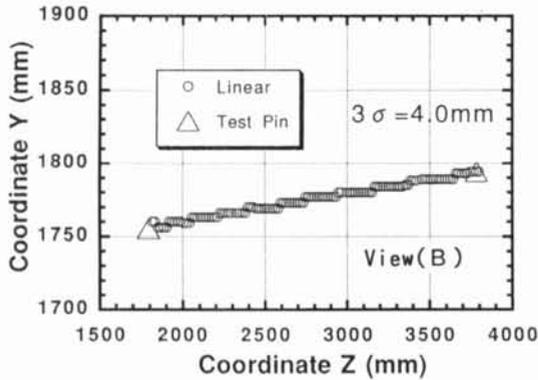
Fig. 9 Measurement Results of Linear Target
Located along the Construction Gauge

CCD sensor resolution $16\,\mu$m. A variation of the value for each view is considered to be caused by calibration errors of test pins(above ②).

In order to practically estimate the validity of the calibration, linear targets were measured. The linear target is furnished with a 2 m long linear test face and located along the boundary of the construction gauge in each view. Fig. 9 shows the results in the views of (A), (B)and(C) respectively. The 3-σ dispersion of ($y_e - y_r$) was below 5 mm in each view, as listed in Table.1, although the dispersion became near 10 mm in cases of inside and outside end of each view. These values are considered to contain all random errors missed at the calibration. Thus, it can be concluded that the calibration was succesfully performed and the static errors for judgement of inversion are reduced to below 5 mm.

Dynamic Errors : The image sensors for the view (D_1)and(D_2) are equipped with conventional telephoto imaging lenses and detect laser-sectional profiles of rails in a high resolution of about 0.4mm. Therefore, from the eq. (1)and(2), the resolutions of dynamic displacement become $\Delta Y_d = 0.4$mm, $\Delta Z_d = 0.6$mm.

The resolution of dynamic rolling angle can be estimated to be $\Delta\theta_r = 2 \cdot \Delta Z / D = 0.9$ mrad. Here, $D = 1067$mm is the distance between rails. The most significant effect from the rolling fluctuation is the errors of Y-value. The magnification of the error is denoted by $\Delta Y_r = \Delta\theta_r \cdot Z$ and estimated to 5 mm at a point of Z = 5.3m high, where range error becomes largest. So, it can be said that a resolution of the dynamic error calibration is below 5 mm.

Field Test : The in-motion measurements was performed for facilities on the Chuo Line at running speeds up to 40km/h. Fig. 10 shows a graphic output on a CRT monitor of the data processor. A tunnel profile data is indicated with the construction gauge. A portion, sticking out into the inside of the tunnel at the top of the curve, indicates a railway contact wire. The curve is broken in the bottom areas because the faces of the tunnel are out of the

Fig. 10
Graphic Display
Tunnel Profile
Data and the
Construction
Gauge
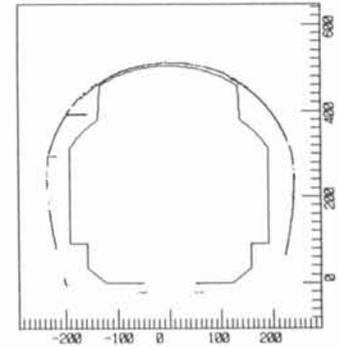
views (C). The view width is contracted there in order to measure the platform profiles in higher resolution than tunnels.

CONCLUSIONS

The authors developed a in-motion obstacle-detecting system for railway surroundings based on an advanced laser-sectioning method. The system obtaines several advantages for use in practical railway inspection along the above mentioned guidelines. Moreover, it was confirmed that the static accuracy for the inspection is better than 5 mm and the resolution of the dynamic error correction is better than 5 mm.

REFERENCES
[1] H. Sasama, 'Application of Image Processing for Railways' Instrumentation and Automation, vol. 19, No. 7 (1991) pp. 53-60
[2] S. Yamamoto and O. Ozeki, '3-D Shape Measurement and Inspection with Structured Light' JSPE, vol. 56, No. 8 (1990) pp. 11-14
[3] S. Hata, 'Identification of 3-D Objects in Industorial Apllication' O plus E, No. 126 (1990) pp. 111-118
[4] K. Mishima et. al, 'Development of Practical Tunnel Profile Measurement System' Annual Report of Okumura Corp. Technical Reseach Institute, No. 17 (1991) pp. 139-144
[5] K. Nakagawa, S. Kanamaru and T. Yamazaki, 'Electrically Inspecting Vehicles for Conventional Railways' Railway and Electrical Engineering, vol. 2 vol. 2, No. 5 (1991) pp. 11-19
[6] S. Kitaori, 'Management of Tunnel Sectional Profiles using Personal Computer' J. Japan Railway Civil Engineering Association, No. 5 (1990) pp. 376-379
[7] T. Ukai, 'Rail Doctor ; Rail Crack Searching Vehicle RFD' Railroad Fan, No. 11 (1991) pp. 81-83
[8] Y. Nakano, et. al, 'Development of the Measuring System for the Distance between Track Centers' Advanty Symposium (V), Proceeding (1992) pp. 21-24
[9] Y. Jin, et. al, 'Dynamic Obstacle-detecting System for Railway Surroundings using a Highly Accurate Laser sectioning Method' IECON'91, vol. 3 (1991) pp. 2426-2430
[10] Y. Goto, et. al, 'Obstacle-detecting System for Railway Surroundings using a Light-sectioning Method Ⅲ' SICE '92 Domestic Session (1992) pp. 147-148